Special Feature: Advanced Alloy Design and Processing of Metallic Materials for Weight- and Energy-saving of Automobiles

Research Report

Microstructure and Wear Resistance of Cu Alloys with Liquid Immiscibility for Laser-clad Valve Seat

Kouji Tanaka, Hajime Kato, Tadashi Oshima and Natsuki Sugiyama

Report received on Apr. 25, 2018

ABSTRACT A new Cu–Ni–Fe–Mo–Si alloy has been developed for a laser-clad valve seat application. During melting of alloy powders by laser processing, the immiscible liquid separated into spherical liquid droplets (L_2) and remaining liquid phase (L_1). The L_2 phase solidifies and transforms to hard grains. The calculated equilibrium L_2 fractions were well correlated with the area fraction and size of hard grains observed in clad beads.

An increase in Mo content increased both the area fraction and maximum grain size, whereas an increase in Ni content had an adverse effect on the grain size. The wear resistance was found to be strongly dependent of the hard grains and proved controllable based on the thermodynamics of liquid immiscibility.

KEYWORDS Laser Cladding, Liquid Immiscibility, Cu Alloys, Solidification, Hard Phase, Wear Resistance

1. Introduction

Power units hybridized with electric motors have rapidly achieved widespread application in daily-use vehicles. With this trend, fuel-efficient combustion technologies are advancing remarkably in terms of improved thermal efficiency. Efficient combustion is achieved in part by enhancing intake tumble flow and depends on the inlet port design.[1] However, the port is usually furnished with a valve seat, i.e., a press-fit wear resistant ring made of hardened steel, which imposes difficulties in optimal port design. In 1991, the Toyota Motor Corporation developed a method for forming valve seats through the direct deposition of raw metal powders and CO_2 laser irradiation.[2] The raw powders were deposited onto the cylinder head, followed by machining into thin walls without possible interference from a press-fit seat ring.

Figure 1[3] shows cross sections of the conventional and newly designed cylinder heads. The laser clad valve seat (LCVS) made possible an ideal straight port with a much lower intake resistance.[3] With increasing the power of the semiconductor laser as a backdrop, the authors have recently launched new cladding facilities and increased the productivity of LCVS production.[1] In addition, a wear-resistant alloy has been developed to meet the requirements of high durability and low cost for global applications.

The developed Cu-Ni-Si base alloy enabled the combination of high thermal conductivity, elevated-temperature strength, and good weldability with aluminum substrate. Here, weldability indicates that cladding is possible at low laser powers, so as to avoid excess alloying and ensure the required bond strength while avoiding detachment. Therefore, the LCVS premises the Cu-based alloy for its high weldability. Bulk heat treatments of the cylinder head

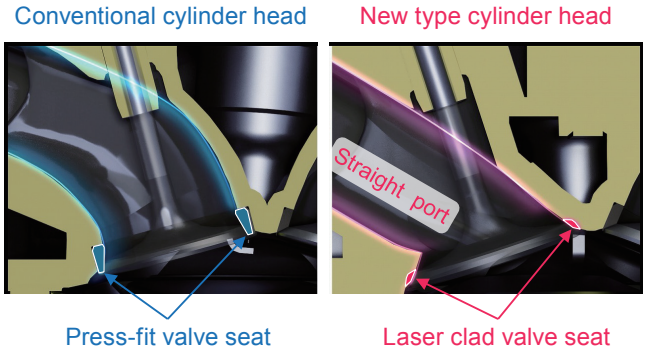

Fig. 1 Comparison of cross section of conventional and newly designed cylinder head.

were not practical for achieving wear resistance by precipitation of fine particles, such as those in Cu-Cr and Cu-Ti alloys. Strengthening of the deposited layer has been more commonly investigated by mixing hard particles, such as chromium carbide[4] and tantalum boride,[5] in Cu alloy powders. In most cases, the wear resistance of the particle-dispersed layer is improved by increasing the fraction of reinforcements.

Conventional microstructures of the press-fit valve seat are usually composed of hard compounds and lubricating soft metals embedded in a high-toughness steel matrix. The raw powders contain carbide particles having a diameter of a few tens of microns and diminish adhesive wear, which becomes severe at elevated temperatures.[6] However, in laser deposition, the temperature of molten metal is raised to more than 2000°C, and the mixed hard powder would also be resolved. As such, the molten metal is likely to be solidified within one second. The crystallized particles from the fast cooling melt are usually very fine. The question is how to include coarse hard grains within a few seconds of fusion and deposition.

Cu alloy systems, such as Cu-Fe systems, have positive mixing enthalpies even at high temperatures and may experience liquid immiscibility (LIM) during rapid cooling. Nagase[7] predicted the occurrence of LIM in an Fe-M-Si-B (M = Cu, Ag, Sn) system based on the binary mixing enthalpies. The LIM has been reported to be stabilized thermodynamically by Si addition to Cu-Fe alloys.[8] Moreover, Cu-Fe, a monotectic Cu-Mo system, also has a stable LIM region.

The isothermal phase diagram of the Fe-Mo-Si system[9] revealed stable compounds, in which Laves ($MgZn_2$ type) and μ (Fe_7W_6 type) phases were both significantly substituted by Si. In a previous study,[10] the thermodynamic calculation predicted the liquid immiscible region and resulting hard phases caused by the additions of Mo, Si, and Ni to a Cu-Fe system. The CALPHAD methodology played a leading role in interpreting the liquid separation, which was difficult to observe directly during the laser deposition process.

In view of the high performance of the LCVS, large hard grains would be required in order to enhance the high-temperature wear resistance of the Cu alloy. The objectives of the present paper are (1) to review the role of the alloying elements on the LIM in the Cu-Ni-Si base alloys and (2) to verify the wear properties in relation to the size of hard grains.

2. Thermodynamic Calculation of Constituent Phase in the Cu-Ni-Fe-Mo-Si System

Both high hardness and compatibility with the mating valve material are required for repeatedly contacting valve seats. The "Corson" Cu-Ni-Si alloy has been selected as the base matrix, where Ni and Si were intended to improve the elevated-temperature strength by solid solution and precipitation hardening.

The composition and fraction of the second liquid (L_2) depend on the thermodynamics of the LIM, which evolves into solute-rich spheres through nucleation and growth. Therefore, if the positive interaction energy in the Cu-Fe liquid is increased with the addition of a third element X, then a larger LIM region and the formation of larger L_2 grains are expected in a ternary Cu-Fe-X system.

2. 1 Thermodynamic Database

A thermodynamic database was assembled for the calculations of the Cu-Ni-Fe-Mo-Si multicomponent system. The molar Gibbs energies of the pure elements and the interaction parameters were obtained from the standard SGTE database.[11] The interaction parameters for the Cu-Ni-Si, Cu-Fe-Si, and Cu-Fe-Mo ternary systems were amended based on recent optimizations.[12-19] Intensive assessments of the μ and Laves phases, which had been performed for the intermetallic compounds in heat-resistant steels, were also introduced in the database.[20] Other minor compounds included were R, P, and σ phases in binary Fe-Mo, iron silicides (*e.g.*, Fe_5Si_3 and FeSi), nickel silicides (*e.g.*, Ni_5Si_2 and Ni_3Si), molybdenum silicides (Mo_5Si_3 and Mo_3Si), and many other copper silicides.

2. 2 Thermodynamic Calculation for the Cu-Ni-Fe-Mo-Si System

2. 2. 1 Liquid Immiscibility

According to the calculated Cu-Fe-Mo diagrams,[15] the LIM occurs at temperatures higher than 1600 K. However, for example, in Cu-10Mo-10Fe (the alloy compositions are given in wt% unless specified otherwise), liquid separation takes place just below 2500 K, which is too high to control the entire separation process with practical laser processing.

Figure 2 shows the multicomponent vertical phase

diagram for the Cu-Ni-Si-Fe-Mo system. The origin denotes the matrix composition (Cu-18Ni-3Si), and the Fe content increases with the fixed atomic Fe/Mo ratio of 2.0. The maximum LIM temperature was 2223 K, and the solubility gap becomes larger with descending temperature. Note that the maximum LIM temperature is lower than that calculated for the Cu-Fe-Mo system[15] and is similar to that calculated for the Cu-20Fe-3Si alloy.[14] Considering the relatively high concentration of Mo at the hemisphere center, the addition of Ni is most likely to decrease the maximum LIM temperature.

Based on the phase equilibrium between L_1 and L_2, numerous L_2 droplets are nucleated from alloys having compositions located far from the $L_1/(L_1 + L_2)$ boundary. Clearly, the phase diagram reveals that the combined increase of Fe and Mo makes the LIM region larger in both composition and temperature. In contrast, further addition of Ni was predicted to have an adverse effect on the LIM region. The calculation on these alloying effects configures strategies for controlling the amount of L_2 droplets.

2. 2. 2 Solidification during Rapid Cooling

Tracking the solidification route of L_2 in Fig. 2, the μ phase is the primary crystal for Fe content exceeding 7.5%, and the remaining L_2 solidifies in eutectic manner with an f.c.c. solid solution and one of the γ (Ni_5Si_2), ρ (Mo_3Si), or σ phase, depending on the total Fe + Mo content. These solid phases consume all of the L_2 below 1223 K, and hard phases present in the alloy with less than 20% Fe are Laves phase and γ. Considering the close composition ranges of the two compounds,[9] it is presumed that the preceding formation of μ, $(Fe,Si)_7Mo_6$, takes place in L_2 and then transforms to Laves phase, $(Fe,Si)_2Mo$, during cooling after solidification.

Starting with roughly 15 vol% hard spheres, the equilibrium phase fraction-temperature diagram was calculated, as shown in **Fig. 3**, for an exploratory alloy composition: Cu-17Ni-10Fe-7Mo-3Si. The figure reveals that LIM starts at 2037 K. Considering the corresponding change of the phase fractions, the evolution sequence of the hard grains is proposed as follows:

(1) Nucleation of L_2 in homogeneous liquid and growth to form spherical droplets.

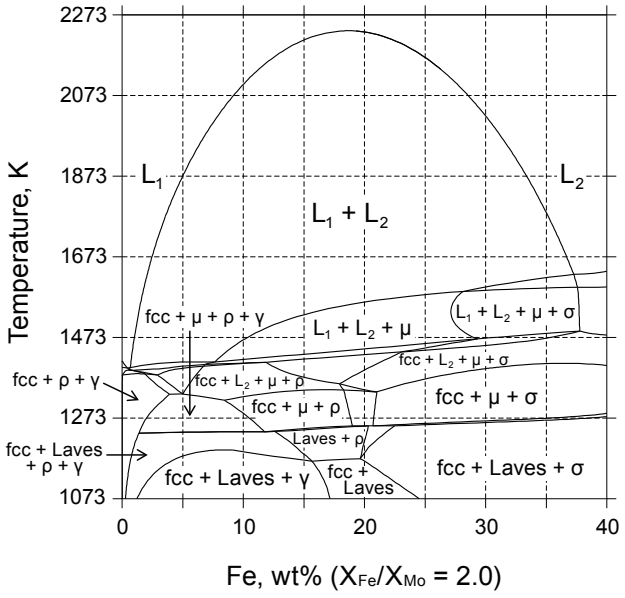

Fig. 2 Vertical phase diagram for Cu-Ni-Si-Fe-Mo system. The origin denotes the matrix composition (Cu-18Ni-3Si) and Fe content increases with the fixed atomic Fe/Mo ratio of 2.0.

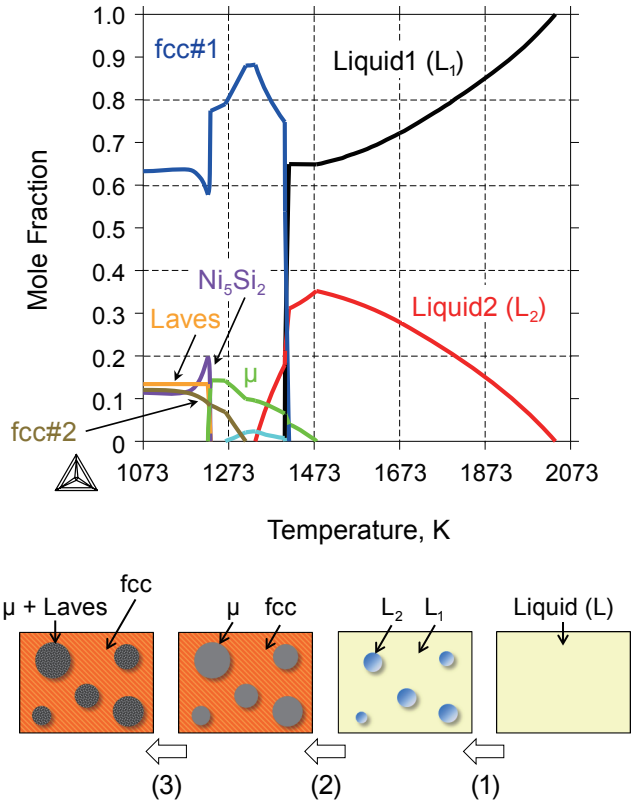

Fig. 3 Calculation equilibrium fraction of phase in Cu-17Ni-10Fe-7Mo-3Si. Sequence (1) to (3) are referred in text.

(2) L_1 solidifies in eutectic manner with an f.c.c. solid solution, and solidification of L_2 spheres having μ precipitates.
(3) Transformation of μ precipitates to Laves phase.

3. Experimental Procedures

3. 1 Microstructure of Laser-deposited Cu-Ni-Fe-Mo-Si Alloys

More than ten Cu-Ni-Fe-Mo-Si alloy powders were prepared by gas atomization and were sieved to 45 to 150 μm in diameter. In order to confirm the liquid separation, one of the powders was melted in an infrared radiation furnace under an argon atmosphere, and the melting surface was observed by laser microscopy. The heating rate was controlled approximately linearly at 100 K/s, and the cooling rate from 1773 to 1273 K was approximately 1 K/s.

Deposited microstructures were investigated for laser-clad specimens. The powders were fed onto an AA5052 aluminum alloy plate in lines, melted, and deposited by the radiation of a direct diode laser (λ = 940 nm) at a power of 3 kW and a scanning speed of 12 mm/s. The clad bead had an angle section of approximately 6 to 8 mm in width and 4 to 6 mm in height. The microstructures were observed by optical microscopy at magnifications of from 50 to 200 times. The dimensions of the hard grains were determined by measuring the area fraction and the maximum hard grain size observed in three fields of view. Constituent phases of the hard grains were analyzed in greater detail by scanning electron microscopy (SEM) and energy-dispersive spectroscopy (EDS).

3. 2 Evaluation of Wear Resistance at Elevated Temperature

Wear resistance of the deposited alloy at elevated temperatures was evaluated by an abrasive wear tester,[2] taking the operation conditions of the intake valve seats into account. The test pieces (3 × 24 × 10 mm) were cut out of laser deposited AA5052 plates. The deposited surface was polished flat and thrust into the polished end face of cylindrical valve material (SUH3: martensitic heat resistant steel) at a loading stress of 9 MPa. The cylinder was then rotated at a circumferential speed of 0.3 m/s, and the temperature of the contact surface was controlled to be constant at 473 K by induction heating. The wear resistance was evaluated based on weight loss after testing for 1.8 ks.

4. Experimental Results and Discussion

4. 1 Observation of Liquid Immiscibility

Figure 4 shows snapshots of the melt surface of a series of Cu-Ni-Fe-Mo-Si alloys. Upon cooling from 1773 K, fine droplets started to nucleate at approximately 1740 K (temperature at the back of the bottom of the crucible) and migrated in one direction as they grew larger until reaching 1673 K. The droplets were adrift only on the uncovered melt, showing no interaction with floating oxide slag. Based on these observation, the droplets are believed to have been captured in-situ during liquid separation.

Because of the indirect temperature measurement, no comparison has been made with the calculation of the LIM region. In laser cladding, the cooling is much faster, and the L_2 spheres have very little time before

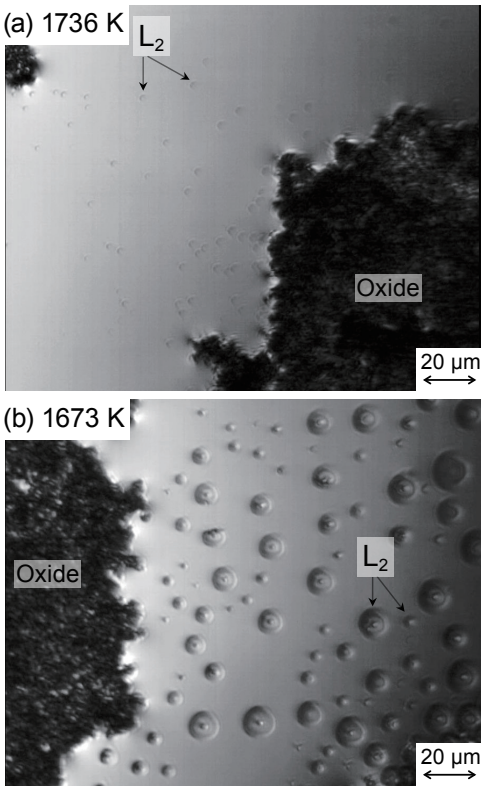

Fig. 4 Laser microscopy image of liquid immiscibility in Cu-Ni-Fe-Mo-Si alloy. Temperature at the back of the crucible is (a) 1736 K and (b) 1673 K.

the overall solidification, which means that they did not always form perfectly spherical grains.

4. 2 Hard Phases in Coarse Grains

Since the Laves phase has the original stoichiometry of A_2Mo, the atomic fraction of Mo has been carefully chosen with respect to the possible elements for A: Fe, Si, and Ni. The tentative composition is Cu-17.2Ni-9.1Fe-6.6Mo-2.9Si. A cross section of the clad bead is shown in **Fig. 5**(a). Numerous coarse grains having diameters of a few tens of microns are distributed in the Cu alloy matrix (Fig. 5(b)). Fig. 5(c) shows a backscattered electron image obtained by SEM for a highly packed structure inside coarse grains. The observed grain consists of two types of fine particles. Semi-quantitative chemical analysis results for each type of particle by EDS are listed in the table in Fig. 5, based on the average composition at five detection points. The Mo concentrations in white particles are close to 46 at%, corresponding to the stoichiometry of the μ phase, $(Ni, Fe, Si)_7Mo_6$, whereas the Mo concentrations in light-gray particles are fixed to 34 at%, which indicates the Laves phase, $(Ni, Fe, Si)_2Mo$.

United outlines of the two phases (μ and Laves) are nearly dendritic, and most of the μ phase is surrounded by a granular Laves phase, suggesting that, the μ phase initially precipitates in L_2 droplets and then transforms to the Laves phase by peritectic reaction with the remaining liquid. Such microstructure evolution of the coarse grain agrees well with the predicted sequence described in Sec. 2. 2. 2.

4. 3 Effects of Mo and Ni on Wear Resistance

The durability of LCVS is to be improved taking the use of an alcohol-petroleum fuel mixture into account. An increase in hard grain fraction would be inevitable, and the effect of alloying elements on the dimensional change in clad microstructures and wear properties should be clarified.

Assuming that the separated liquids instantly attain equilibrium fractions at each temperature during cooling, it is reasonable to estimate the fraction of hard grains with reference to the equilibrium L_2 fraction at temperatures just above the overall solidification. **Figure 6** shows the correlation between the calculated L_2 fraction and the area fraction of coarse grains. The measurements have been carried out on the clad microstructures whose average compositions were varied in the range of Cu-(15.9-18.4)Ni-(7.2-9.6)Fe-(6.0-9.3)Mo-(2.2-3.1)Si. The L_2 fraction is represented by the value of 1673 K, according to the assumption. The linear relationship is

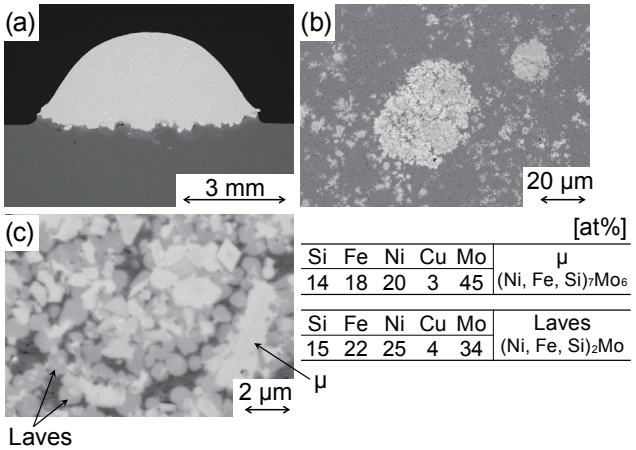

Fig. 5 (a) Back scattered electron image of laser-clad microstructure of Cu-17.2Ni-9.1Fe-6.6Mo-2.9Si. (b) Back scattered electron image of the corse grain. (c) Magnified image of the corse grain. Average composition (at%) of gray particles are summarized in table.

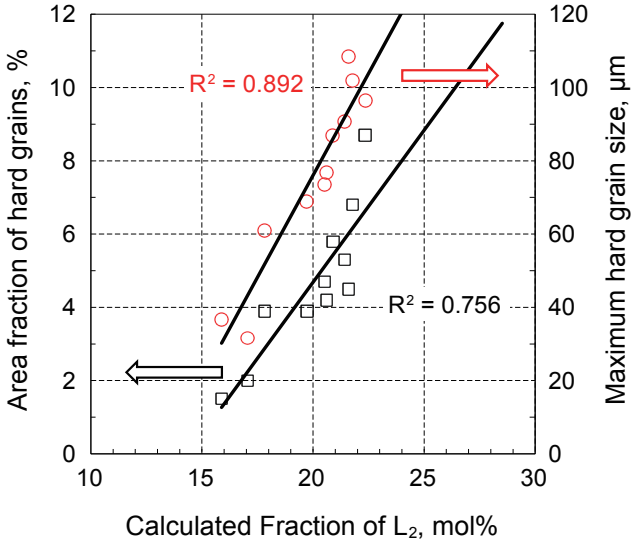

Fig. 6 Correlation of calculated L_2 fraction with dimensions of coarse grain measured in clad microstructures.

useful for plotting the area fraction of coarse grains, which is approximately one-quarter of the calculated L_2 fraction. In addition, a better correlation is found with the maximum hard grain size. Thus the coarseness of the grains is phenomenologically "*controllable*" using the L_2 fraction as an index calculated from alloy chemistry.

The chemical compositions of the wear test samples are shown in **Table 1**, and the clad microstructures of the four alloys are shown in **Fig. 7**. As the Mo content increase from 6% in Fig. 7(a) to 10% in Fig. 7(c), extraordinarily coarse grains become involved in microstructures. However, this is accompanied by a decrease in Ni content, and, therefore, the relationship between the Mo/Ni weight ratio and the maximum hard grain size is also given in Fig. 7(e). For a ratio of less than 0.50, the maximum hard grain size increases linearly. However, at a ratio of 0.70, the maximum hard grain size is 200 μm greater than the linearly extrapolated value, and the Si content may also decrease slightly. Therefore, the addition of Mo results in large grains, and the simultaneous increase in Ni content was found to be important for eliminating excessively large grains.

The weight loss after wear testing with respect to measured area fraction is summarized in **Fig. 8**. It is evident that the larger the area fraction is, the smaller the wear loss becomes. In general, for composite materials, the fraction of hard phase determines the average hardness, and thus the wear resistance in abrasive sliding. The 20%Ni alloy in Fig. 7(d) showed poor wear resistance, despite the area fraction of hard grains being as high as that of the 10%Mo alloy.

The tribological advantage of the "coarseness" of hard grains is not necessarily recognized, or rather it has been reported to be inferior to fine particles in room-temperature sliding. For example, submicron-order carbide contributes to a smaller wear rate of composite compared to carbide on the order of a few microns.[20,21] Finer particles of the same fraction reduce the inter-particle distance, which prevents the matrix alloy from being removed through wear. In contrast, SiC particles of more than 15 μm were superior to the same fraction of 2.4 μm particles in low-load sliding, where hard phases act as load-bearing constituents.[22] For present-day clad alloy, the size of hard grains ranges to more than 200 μm. The largest group of grains may carry the entire load after slight wear in the matrix and inhibits further wearing of the material. In addition, owing to

Table 1 Chemical composition of alloys used for the wear test.

[wt%]

	Cu	Ni	Fe	Mo	Si	Mo/Ni
(a)	bal.	17.2	9.1	6.6	2.9	0.38
(b)	bal.	17.2	9.2	7.9	3.1	0.46
(c)	bal.	15.0	8.3	10.5	2.4	0.70
(d)	bal.	20.0	7.8	10.0	3.4	0.50

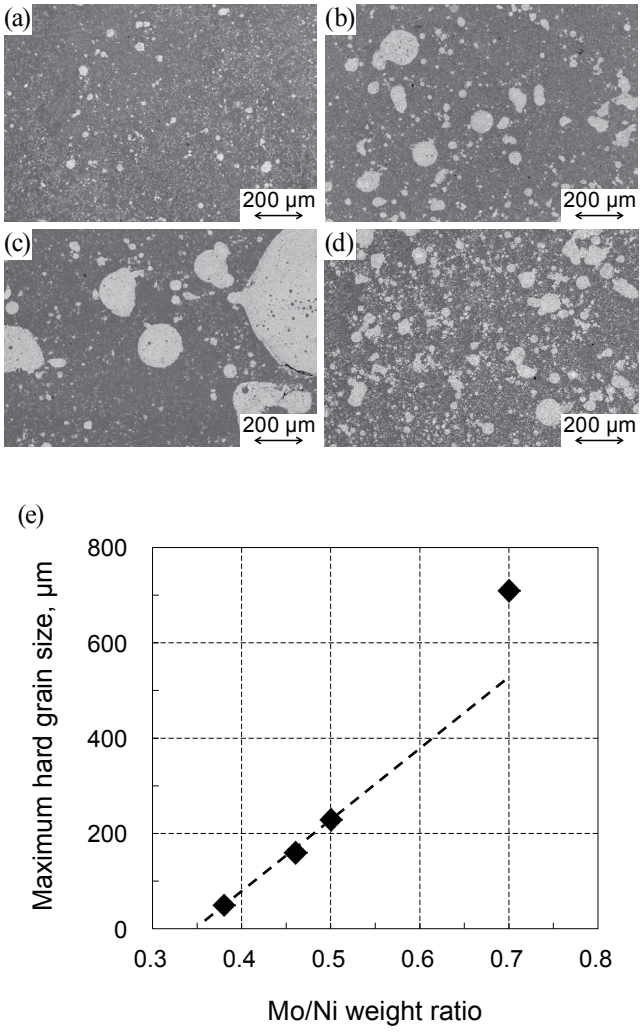

Fig. 7 Microstructures of clad alloys used for the wear tests. (a) Cu-17.2Ni-9.1Fe-6.6Mo-2.9Si, (b) Cu-17.2Ni-9.2Fe-7.9Mo-3.1Si, (c) Cu-15.0Ni-8.3Fe-10.5Mo-2.4Si, (d) Cu-20.0Ni-7.8Fe-10.0Mo-3.4Si (mass%) (e) Relationship between Mo/Ni weight ratio and maximum hard grain size.

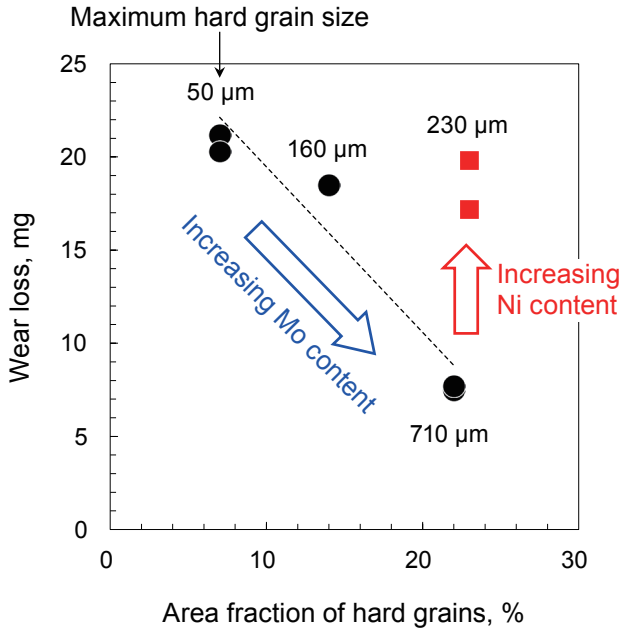

Fig. 8 Effect of hard grains on wear resistance.

the agglomerated fine compound structure, as shown in Fig. 5(c), coarse hard grains are considered to be difficult to break or chip off.

5. Conclusions

Liquid immiscible Cu alloys were developed for direct deposition in the manufacturing of a laser-clad valve seat. CALPHAD thermodynamic analysis predicted the liquid immiscibility to occur at temperatures below 2037 K in Cu-17Ni-10Fe-7Mo-3Si alloy, which was confirmed by in-situ observations. In a clad bead of the quinary alloy, coarse hard grains were incorporated as solidification products of separated liquids. As predicted based on the stable phase in an Fe-Mo-Si system, the coarse grain consisted of an agglomeration of hard phases, i.e., μ and Laves phases.

The equilibrium fraction of the separated liquid at 1673 K was correlated well with the dimensions of coarse grains in various Cu-Ni-Fe-Mo-Si alloys. The increase in Mo content linearly increased the area fraction and maximum hard grain size. On the other hand, the increase in Ni content eliminated the largest group of grains, and such a refined microstructure was proved unfavorable in terms of wear resistance under test conditions of 9 MPa at 473 K.

References

(1) Aoyama, H., Kawasaki, M., Miyara, N., Sugiyama, N., Ando, K., Yanaka, K. and Oshima, T., "Development of Laser Clad Valve Seat", *Proc. JSAE Annu. Spring Congr.* (in Japanese), No. 69-17 (2017), pp. 1854-1859.

(2) Tanaka, K., Saito, T., Shimura, Y., Mori, K., Kawasaki, M., Koyama, M. and Murase, H., "New Copper Based Composite for Engine Valve Seat Directly Deposited onto Aluminium Alloy by Laser Cladding Process", *J. Jpn. Inst. Metals*, Vol. 57, No. 10 (1993), pp. 1114-1122.

(3) Toyota Motor Corporation, "New 2.5-liter Direct-injection, Inline 4-cylinder Gasoline Engine", *TOYOTA Global Newsroom*, <https://newsroom.toyota.co.jp/en/powertrain/engine/>, (accessed 2018-04-18).

(4) Zhang, L., Elias, A., Chen, W. and Gao, K., "Electrical Conductivity and Wear Behavior of Bi-continuous Cr_3C_2-Cu Composites", *Ceramics International*, Vol. 41, No. 9, Part A (2015), pp. 11075-11079.

(5) Ichikawa, K. and Achikita, M., "Effect of Heat Treatment on Mechanical and Electrical Properties of Compocast Dispersion-strengthened Coppers", *J. Jpn. Inst. Metals*, Vol. 57, No. 11 (1993), pp. 1310-1316.

(6) Kawata, H. and Fujitsuka, H., "Co, Pb-free Exhaust Valve Seat Insert Material", *Hitachi Chem. Tech. Report* (in Japanese), No. 44 (2005), pp. 31-34.

(7) Nagase, T., Suzuki, M. and Tanaka, T., "Microstructure of Rapidly Solidified Fe-M-Si-B (M = Cu, Ag, Sn) Immiscible Alloys", *J. Soc. Mater. Sci. Jpn.*, Vol. 64, No. 3 (2015), pp. 175-182.

(8) Wang, C.-P., Liu, X.-J., Ohnuma, I., Kainuma, R. and Ishida, K., "Formation of Immiscible Alloy Powders with Egg-type Microstructure", *Science*, Vol. 297, No. 5583 (2002), pp. 990-993.

(9) Villars, P., Prince, A. and Okamoto, H., *Handbook of Ternary Phase Diagrams* (1995), pp. 10482-10487, ASM International.

(10) Tanaka, K., Kato, H. and Oshima, T., "Design of Laves-phase-packed Spheres in Wear-resistant Cu Alloy by Controlled Liquid Immiscibility", *CALPHAD*, Vol. 58 (2017), pp. 50-57.

(11) Dinsdale, A. T., "SGTE Data for Pure Elements", *CALPHAD*, Vol. 15, No. 4 (1991), pp. 317-425.

(12) Chen, Q. and Jin, Z., "The Fe-Cu System: A Thermodynamic Evaluation", *Metall. Mater. Trans. A*, Vol. 26, No. 2 (1995), pp. 417-426.

(13) Miettinen, J., "Reassessed Thermodynamic Solution Phase Data for Ternary Fe-Si-C System", *CALPHAD*, Vol. 22, No. 2 (1998), pp. 231-256.

(14) Wang, C.-P., Liu, X.-J., Ohnuma, I., Kainuma, R. and Ishida, K., "Phase Equilibria in Fe-Cu-X (X: Co, Cr, Si, V) Ternary Systems", *J. Phase Equil.*, Vol. 23, No. 3 (2002), pp. 236-245.

(15) Wang, C.-P., Liu, X.-J., Ohnuma, I., Kainuma, R., Hao, S.-M. and Ishida, K., "Phase Equilibria in the Cu-Fe-Mo and Cu-Fe-Nb Systems", *J. Phase Equil.*, Vol. 21, No. 1 (2000), pp. 54-62.
(16) Brewer, L. and Lamoreaux, R. H., *Atomic Energy Rev., Spec. Iss.*, No. 7, (1980), pp. 236-238, International Atomic Energy Agency.
(17) Andersson, J.-O., "A Thermodynamic Evaluation of the Fe-Mo-C System", *CALPHAD*, Vol. 12, No. 1 (1988), pp. 9-23.
(18) Wang, C., Zhu, J., Lu, Y., Guo, Y. and Liu, X., "Thermodynamic Description of the Cu-Ni-Si System", *J. Phase Equil. Diffus.*, Vol. 35, No. 1 (2014), pp. 93-104.
(19) Liu, Y., Shao, G. and Tsakiropoulos, P., "Thermodynamic Reassessment of the Mo-Si and Al-Mo-Si Systems", *Intermetallics*, Vol. 8, No. 8 (2000), pp. 953-962.
(20) MatCalc Engineering, "MatCalc Open Databases", *MatCalc Engineering*, <https://www.matcalc-engineering.com/index.php/matcalc-databases/matcalc-databases-sub>, (accessed 2018-04-18).
(21) Yang, Q., Senda, T. and Ohmori, A., "Effect of Carbide Grain Size on Microstructure and Sliding Wear Behavior of HVOF-sprayed WC−12% Co Coatings", *Wear*, Vol. 254, No. 1-2 (2003), pp. 23-34.
(22) Garcia, I., Fransaer, J. and Celis, J.-P., "Electrodeposition and Sliding Wear Resistance of Nickel Composite Coatings Containing Micron and Submicron SiC Particles", *Surf. Coat. Technol.*, Vol. 148, No. 2-3 (2001), pp. 171-178.
(23) Alpas, A. T. and Zhang, J., "Effect of Microstructure (Particulate Size and Volume Fraction) and Counterface Material on the Sliding Wear Resistance of Particulate-reinforced Aluminum Matrix Composites", *Metallur. Mater. Trans. A*, Vol. 25, No. 5 (1994), pp. 969-983.

Figs. 4 and 6
Reprinted from CALPHAD, Vol. 58 (2017), pp. 50-57, Tanaka, K., Kato, H. and Oshima, T., Design of Laves-phase-packed Spheres in Wear-resistant Cu Alloy by Controlled Liquid Immiscibility, © 2017 CALPHAD, with permission from CALPHAD.

Kouji Tanaka
Research Fields:
- Metallic Materials
- Material Processing

Academic Degree: Dr.Eng.
Academic Societies:
- The Iron and Steel Institute of Japan
- The Japan Society of Heat Treatment

Awards:
- Technical Development Award, The Japan Institute of Metals and Materials, 1996
- R&D100 Award, 1998
- Dissertation Award, Gas Turbine Society of Japan, 2002
- The APDIC Industrial Award, 2018

Present Affiliation: Daido University

Hajime Kato
Research Fields:
- Metallic Materials
- Material Processing

Academic Societies:
- The Japan Institute of Metals and Materials
- The Japan Institute of Light Metals
- The Magnetics Society of Japan

Award:
- The APDIC Industrial Award, 2018

Tadashi Oshima
Research Fields:
- Metallic Materials
- Laser Processing

Academic Societies:
- Japan Welding Society
- Japanese Society of Tribologists

Awards:
- R&D 100 Awards, 1998
- The APDIC Industrial Award, 2018

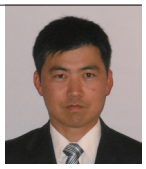

Natsuki Sugiyama*
Research Field:
- Engine Production Engineering Development

Academic Society:
- Society of Automotive Engineers of Japan

*Toyota Motor Corporation

